



Modelling of Hybrid Rocket Flow-Fields with Computational Fluid Dynamics

Izham Izzat Ismail¹, Nur Husnina Aufa Rozainuddin¹, Norhuda Hidayah Nordin², Muhammad Hanafi Azami^{1,*}

¹ Department of Mechanical & Aerospace Engineering, Faculty of Engineering, International Islamic University Malaysia, Kuala Lumpur, Malaysia

² Department of Manufacturing and Materials Engineering, International Islamic University Malaysia, Kuala Lumpur, Malaysia

ARTICLE INFO

Article history:

Received 14 August 2021

Received in revised form 11 March 2022

Accepted 12 March 2022

Available online 31 March 2022

Keywords:

Hybrid rocket flow fields; CFD modeling; GOX paraffin; N2O paraffin

ABSTRACT

A low regression rate is a major limitation in the hybrid rocket propulsion system. This paper is to study the regression rate characteristics of a cylindrical solid grain with cryogenic propellants. Paraffin (P) fuel is coupled with two types of oxidizers, namely gaseous oxygen (GOX) and nitrous oxide (N2O). ANSYS software is used as the CFD platform to observe the hybrid rocket flow-fields. The modelling values obtained from the pressure, temperature, velocity, and wall heat flux contours are used to calculate the hybrid rocket performance in terms of regression rate, thrust, specific impulse, characteristic velocity, and exit Mach number. The numerical results show that the mass-flow-inlet boundary conditions, initial design feature, and type of propellant play an important role in the enhancement of hybrid rocket performance. Result shows that enhanced of 68 % of the regression rate, 59 % of thrust, 6 % of specific impulse and exit Mach number, and % of characteristic velocity by improved 50% of mass flow rate. Due to the high flame temperature, the GOX/P propellants produce the best hybrid rocket motor compared with the others.

1. Introduction

The two most common forms of rocket engines are liquid rockets and solid rockets. The fuel and oxidizer are stored separately as fluids in a liquid rocket and are poured into the nozzle's combustion chamber where the burning takes place. The propellants are combined and loaded into a rigid container in a solid rocket. Nonetheless, rockets differ from conventional air-jet propulsion, such as turbojets and ramjets, because the rocket engine itself contributes all the propellants to the rocket motor [1].

Hybrid rocket engines combine solid fuel with a liquid or gas oxidizer. This type of rocket propulsion is attractive and provides many advantages over conventional liquid or solid rocket propulsion systems due to their low-cost, fuel handling simplicity, durability, throttling capability, and eco-friendly attributes [2-8]. It is easy to throttle the hybrid rocket engines by adjusting the oxidizer mass flow rate, which serves as ideal candidates for adjustable thrust rocket and is appropriate for

* Corresponding author.

E-mail address: hanafiazami@iium.edu.my (Muhammad Hanafi Azami)

all applications where rockets are used [9-12]. This is due to the versatility of the propellant, the wide range of performance, and the flexibility of the thrust [13].

Every regression rate is regarded as the crucial parameter which has the consequences of the first order on the engine design and thus on the engine performance [14,15]. The regression rate is dependent on the oxidizer mass flux rate, indicating that the rate at which the fuel burns is proportional to the amount of oxidizer flowing through the port, according to the governing equation for hybrid rocket combustion. The regression rate of a solid rocket motor is related to the motor's chamber pressure. For its non-premixed diffusion combustion, the fuel regression rate of the hybrid rocket engine is lower than that of the solid rocket engine [15-18]. The hybrid rocket combustion usually occurs in the boundary layer above the surface of the fuel rather than on the surface of the fuel itself [16,19]. It has been studied that member of the usual alkaline group of hydrocarbons, which are solid at room temperature and have low surface tension and viscosity, such as paraffin waxes and polyethylene waxes, are the most appropriate elements in hybrid rocket fuel to generate high regression rates compared to conventional hybrid fuel [20-22].

The hybrid engine design includes a comprehension of the physical forces that control the fuel port combustion processes and fluid dynamics. Computational Fluid Dynamics (CFD) is a fluid mechanics branch that utilizes mathematical modeling and information structures to examine and solve fluid-related problems. It refers to a wide range of research and engineering topics in many fields of study and business, including aerodynamics and aviation modeling, atmospheric prediction, natural science and environmental engineering, combustion analysis, and construction fluid flows [23-25]. CFD enables the theoretical simulation of any physical condition and gives a lot of control over the physical process and allows user to isolate individual phenomena for research [26]. With the usage of the numerical simulation technique, flow-fields, and the instantaneous regression rates can be investigated using various type of operation conditions.

In several areas of space transportation, hybrid rocket propulsion system is considered because it is the best system and has better capacity for environmentally friendly technology. In pursuing hybrid technology and rocket, a country's entry into the space exploration community is an inspiration and a big boost. Therefore, development work and analytical research must be performed in tandem, as it happens in the rocket final level motor progression. The use of different HRM parameters and design has been introduce in order to demonstrate the consequence on the regression rate. This research will aim to focus on obtaining a better performance of hybrid rocket motor.

2. Governing Equations

For low Mach and Reynolds values, the conservation equations for a two-dimensional, unstable, viscous, compressible flow are as follows, and the continuity equation is as follows:

$$\frac{\partial \rho}{\partial t} + \frac{\partial}{\partial x}(\rho u) + \frac{\partial}{\partial y}(\rho v) = 0 \quad (1)$$

In the x-direction, the momentum equation is given by

$$\frac{\partial}{\partial t}(\rho u) + \frac{\partial}{\partial x}(\rho u^2) + \frac{\partial}{\partial y}(\rho uv) + \frac{\partial p}{\partial x} - \frac{\partial}{\partial x} \left[\frac{2}{3} \mu_{eff} \left(2 \frac{\partial u}{\partial x} - \frac{\partial v}{\partial y} \right) \right] - \frac{\partial}{\partial y} \left[\mu_{eff} \left(\frac{\partial u}{\partial y} + \frac{\partial v}{\partial x} \right) \right] = 0 \quad (2)$$

In the y-direction (normal to the fuel surface), the momentum equation is:

$$\frac{\partial}{\partial t}(\rho v) + \frac{\partial}{\partial x}(\rho uv) + \frac{\partial}{\partial y}(\rho v^2) + \frac{\partial p}{\partial y} - \frac{\partial}{\partial x} \left[\mu_{eff} \left(\frac{\partial u}{\partial y} + \frac{\partial v}{\partial x} \right) \right] - \frac{\partial}{\partial y} \left[\frac{2}{3} \mu_{eff} \left(2 \frac{\partial v}{\partial y} - \frac{\partial u}{\partial x} \right) \right] = 0 \quad (3)$$

The effective viscosity in the above equations is defined as

$$\mu_{eff} = \mu + \mu_t \quad (4)$$

where the eddy viscosity is given by

$$\mu_t = \rho C_\mu \frac{K^2}{\varepsilon} \quad (5)$$

The equation of state is given by:

$$p = \rho RT \quad (6)$$

The turbulent kinetic energy is determined from:

$$\frac{\partial(\rho K)}{\partial t} + \frac{\partial(\rho u K)}{\partial x} + \frac{\partial(\rho v K)}{\partial y} = \frac{\partial}{\partial x} \left[\left(\mu + \frac{\mu_t}{Pr_K} \right) \frac{\partial K}{\partial x} \right] + \frac{\partial}{\partial y} \left[\left(\mu + \frac{\mu_t}{Pr_K} \right) \frac{\partial K}{\partial y} \right] + \mu_t \left[\left(\frac{\partial u}{\partial y} + \frac{\partial v}{\partial x} \right)^2 + 2 \left(\frac{\partial u}{\partial x} \right)^2 + 2 \left(\frac{\partial v}{\partial y} \right)^2 \right] - \rho \varepsilon \quad (7)$$

The turbulent dissipation energy is determined from:

$$\frac{\partial(\rho \varepsilon)}{\partial t} + \frac{\partial(\rho u \varepsilon)}{\partial x} + \frac{\partial(\rho v \varepsilon)}{\partial y} = \frac{\partial}{\partial x} \left[\left(\mu + \frac{\mu_t}{Pr_\varepsilon} \right) \frac{\partial \varepsilon}{\partial x} \right] + \frac{\partial}{\partial y} \left[\left(\mu + \frac{\mu_t}{Pr_\varepsilon} \right) \frac{\partial \varepsilon}{\partial y} \right] + C_{\varepsilon 1} \mu_t \frac{\varepsilon}{K} \left[\left(\frac{\partial u}{\partial y} + \frac{\partial v}{\partial x} \right)^2 + 2 \left(\frac{\partial u}{\partial x} \right)^2 + 2 \left(\frac{\partial v}{\partial y} \right)^2 \right] - C_{\varepsilon 2} \rho \frac{\varepsilon^2}{K} \quad (8)$$

The K- ε constants used in this investigation are as follows: $C = 0.09$, $Pr_K = 1.0$, $Pr_\varepsilon = 1.3$, $C_{\varepsilon 1} = 1.55$, and $C_{\varepsilon 2} = 2.0$ [27]. The energy equation is given by:

$$\frac{\partial}{\partial t} \left[(c_p - R) \rho T \right] + \frac{\partial}{\partial x} (c_p \rho u T) + \frac{\partial}{\partial y} (c_p \rho v T) - \frac{\partial}{\partial x} \left(k_{eff} \frac{\partial T}{\partial x} \right) - \frac{\partial}{\partial y} \left(k_{eff} \frac{\partial T}{\partial y} \right) - Q_H w_f = 0 \quad (9)$$

The regression rate of the hybrid rocket motor can be calculated by using the following Eq. (10).

$$\dot{r} = \frac{\dot{q}_{wall}}{\rho_{fuel} h_v} \quad (10)$$

where \dot{q}_{wall} , ρ_{fuel} , and h_v represent wall heat flux, the density of fuel grain, and decomposition heat of fuel respectively. The physical properties of the paraffin wax are shown in Table 1 [28].

Table 1
 Physical properties of paraffin

Density (kg/m ³)	Specific heat (J/kg·K)	Thermal conductivity (W/m·K)	Decomposition heat (cal/kg)
835	2800	0.210	850

Eq. (2) which is the nozzle relations can be used to calculate the rocket thrust. Where \dot{m} , U_e , p_e , p_0 , and A_e represent mass flow rate, exit velocity, exit pressure, ambient pressure, and nozzle exit area. The specific impulse which is a measure of how effectively a rocket uses propellant can be obtained by using Eq. (12).

$$T = \dot{m}U_e + (p_e - p_0)A_e \quad (11)$$

$$I_{sp} = \frac{T}{\dot{m}g} \quad (12)$$

The characteristic velocity is obtained by dividing the product of the pressure chamber, p_c and throat area, A^* with a mass flow rate. Eq. (14) shows the exit Mach number formula used where the specific heat ratio $\gamma = 1.2$ and gas constant $R = 287 \text{ J/kg}\cdot\text{K}$.

$$C^* = \frac{p_c A^*}{\dot{m}} \quad (13)$$

$$M_e = \frac{U_e}{\sqrt{\gamma R T_e}} \quad (14)$$

Additionally, the oxidizer mass flux, G is calculated using Eq. (15) where it is equal at any time to the oxidizer flow rate divided by the combustion port area, A_c .

$$G = \frac{\dot{m}}{A_c} \quad (15)$$

3. Preference Design and Choice Model

In ANSYS Workbench software, Fluent Fluid Flow is chosen as the analysis system to simulate the flow-fields in the hybrid rocket motor. There will be several steps that have to be followed in the project schematic before obtaining the hybrid rocket flow-fields. The working processes in the CFD simulation are geometry, mesh, setup, solution, and result.

3.1 Geometry Selection

The desired system of length units to work from will be prompted to set to millimetres in this scenario. The schematic image of the hybrid rocket motor model is shown in Figure 1 where it consists of the inlet, pre-combustion chamber, paraffin wax surface, sub-combustion chamber, and outlet region. The model is cut into a quarter of its actual geometry by using the symmetry option in the Design Modeler. The reason is to make it easier to observe the flow since the model is symmetrical and to reduce the computation time. The parameter of the hybrid rocket motor parts is listed in Table 2 below.

Table 2
Parameters of hybrid rocket geometry

Parameter	Value (mm)
Diameter of the combustion chamber	35
Diameter of tube grain	13
Diameter of the nozzle throat	3
Expansion area ratio of nozzle	2.5
Fuel grain length	250
Length of the pre-combustion chamber	30
Length of sub-combustion chamber	30

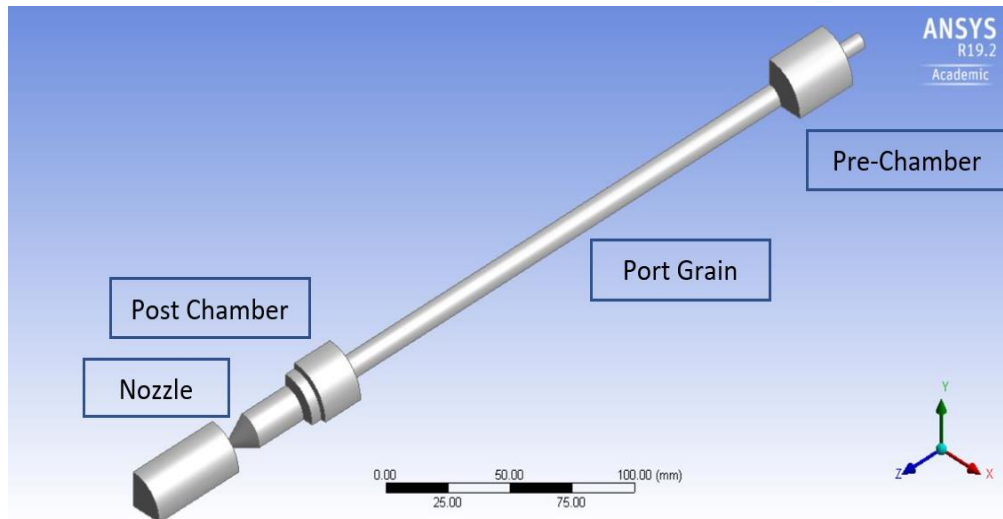


Fig. 1. The geometry of the hybrid rocket motor

3.2 Node and Cell Specification

The statistics of the mesh model in Figure 2 consists of 18523 nodes and 42926 elements. The element order is linear with a size of 4.1 mm. Automatic method and inflation are used in this meshing with high smoothing and orthogonal quality of mesh metric. Thirteen faces are chosen for the boundary in this geometry unit. Inflation choice is full thickness with a peak thickness of 7 layers and 2 mm. The finer the mesh, the better the results. If the mesh is finer across the domain, however, the solvers will need more computation time. Inlet, pre-chamber, paraffin, sub-chamber, outlet, and symmetry are included in the names selections before proceeding to the next step.

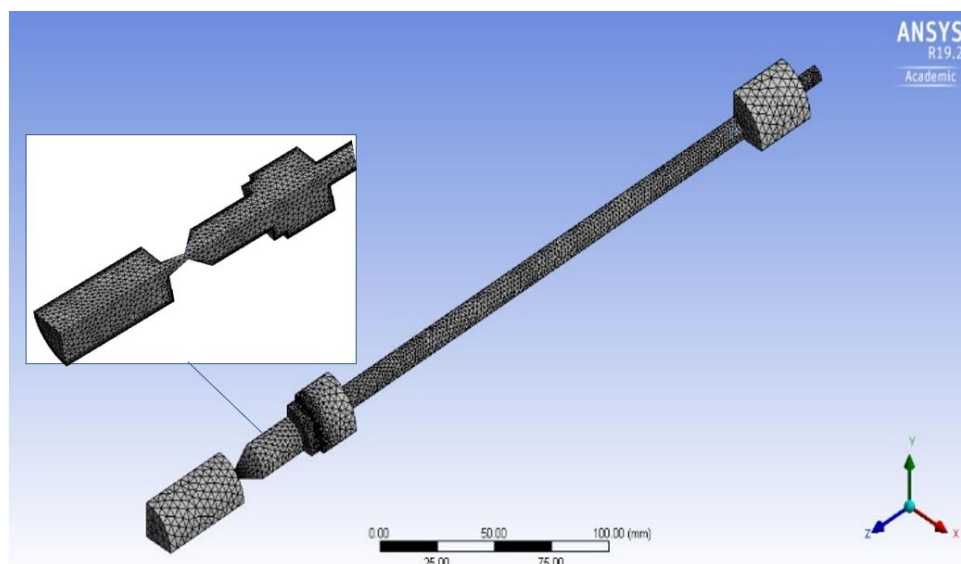


Fig. 2. Meshing structure of the model with zoomed boundary condition

3.3 Modelling Condition

Pressure-based type, absolute velocity formulation, and transient time are selected. The turbulence model is the Large Eddy Simulation (LES) in which each property will be specially averaged. The energy and species transport are also used for the model. The materials consist of solid, fluid, and mixture. The properties of paraffin are entered in the solid part. A fluent database is used to insert the properties of oxidizer either GOX or N₂O, in both fluid and mixture. The boundary type for the inlet is mass-flow-inlet. Table 3 shows the conditions with varying mass flow rate, pressure, and temperature inlet. For paraffin, the wall type is fixed at temperature 550 K. Pressure-outlet is selected for the outlet with a temperature of 300 K and pressure of 1 atm or 101325 Pa.

Table 3
 Hybrid rocket motor modeling conditions

Case	\dot{m} (kg/s)	Pressure (atm)	Temperature (K)	ϵ
1	0.10	2	800	2.5
2	0.15	2	800	2.5
3	0.20	2	800	2.5
4	0.10	3	800	2.5
5	0.10	4	800	2.5
6	0.10	2	1000	2.5
7	0.10	2	1200	2.5
8	0.10	2	800	3.0
9	0.10	2	800	3.5

3.4 Solution

Hybrid initialization is selected. This initialization of hybrids is a collection of recipes and methods of boundary interpolation. SIMPLE scheme, least-squares cell-based gradient, second-order pressure, second-order upwind velocity, bounded central differencing, second-order upwind energy, y, and second-order implicit transient formulation are selected for the solution methods. To run the calculation, the input is as in Table 4.

Table 4
 Solution input to run the calculation.

Time step size (s)	Number of time steps	Maximum iterations	Reporting interval	Profile update interval
0.00005	50	150	500	500

4. Result and Discussion

4.1 Representative Flow-Fields

Four types of contours; pressure, temperature, velocity in Z-direction, and wall heat flux as shown in Figure 3 to Figure 6 for baseline are observed from the hybrid rocket flow-fields obtained in the ANSYS software where these flow-fields are viewed in CFD-Post environment. Based on Figure 3 the flow-fields, the peak pressure is reached in the first quarter of the fuel grain since the geometry size is reduced. The pressure drops drastically at the nozzle throat. The temperature in Figure 4 has the same effect as the pressure. From Figure 5 the velocity is high at the oxidizer inlet and the nozzle throat afterward. The wall heat flux value decreases along the fuel grain in Figure 6. This has a significant effect on the regression rate.

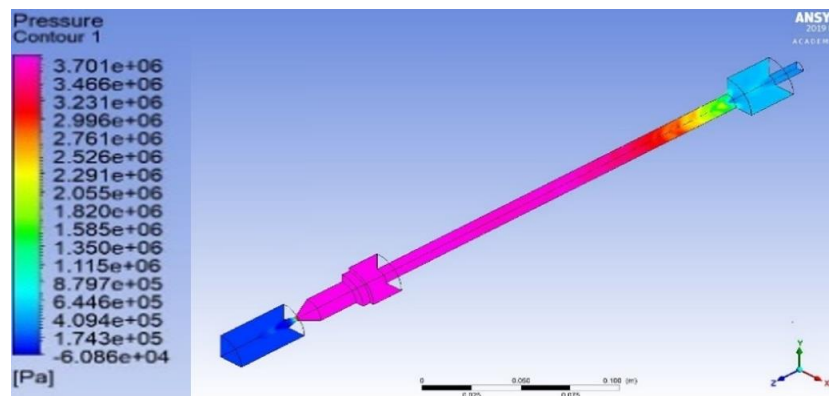


Fig. 3. Pressure contour

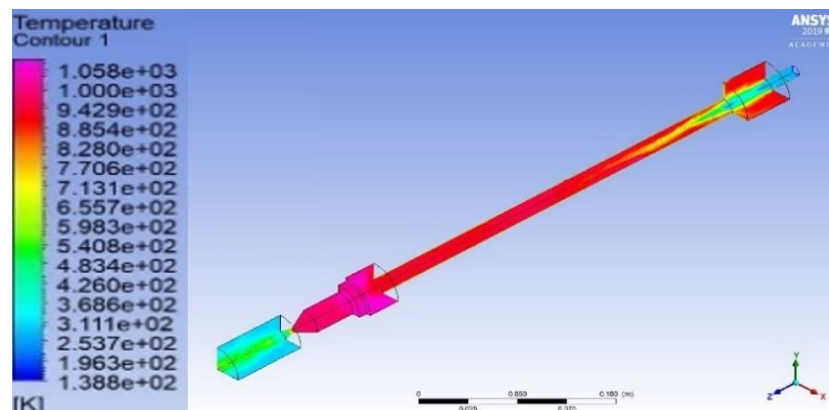


Fig. 4. Temperature contour

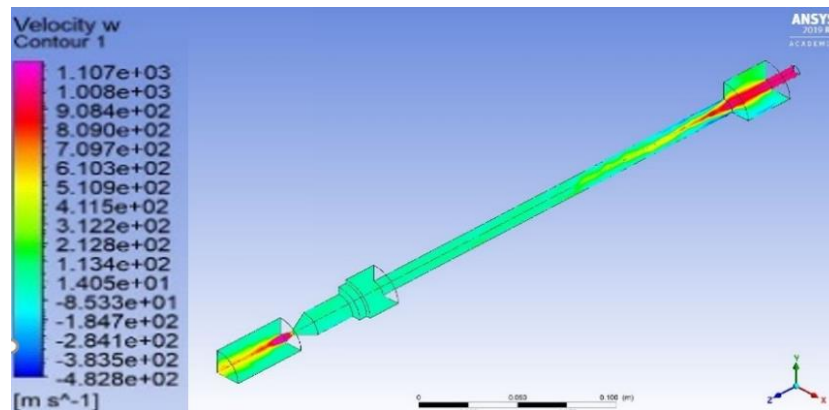


Fig. 5. Velocity contour

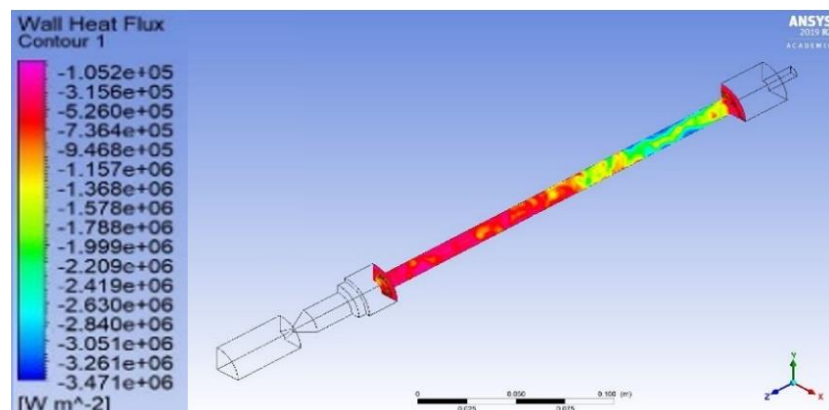


Fig. 6. Wall heat flux contour

4.2 Hybrid Rocket Performance

The performance of the hybrid rocket can be calculated based on the numerical results from the hybrid rocket flow-fields. The modelling values such as average wall heat flux, exit velocity, exit pressure, exit temperature, and chamber pressure for both GOX/P and N2O/P hybrid rocket are shown in Table 5 and Table 6.

Table 5
 Modeling values for GOX/P

Case	$\dot{q}_{wall,ave}$ (Wm ⁻²)	U _e (m/s)	P _e (MPa)	T _e (K)	P _c (MPa)
1	1382168	1107	0.1743	368.6	3.701
2	2291840	1141	0.3138	350.7	5.826
3	3032040	1162	0.4500	343.9	7.888
4	1397092	1110	0.1727	372.0	3.703
5	1448832	1132	0.1639	371.3	3.561
6	2272780	1232	0.2222	437.5	4.366
7	3355680	1357	0.2733	504.0	5.143
8	1407348	1141	0.1632	373.4	3.657
9	1550472	1195	0.1535	374.2	3.802

Table 6
 Modeling values for N2O/P

Case	\dot{q}_{wall_ave} (Wm ⁻²)	U _e (m/s)	P _e (MPa)	T _e (K)	P _c (MPa)
1	1011836	1000	0.1598	369.9	3.313
2	1382368	1025	0.2781	336.7	5.032
3	1999208	1042	0.3781	319.0	6.574
4	1132276	968	0.1408	368.3	3.069
5	1252840	959	0.1365	369.2	3.006
6	1960612	1159	0.1971	431.5	3.796
7	2761800	1307	0.2306	513.1	4.249
8	1370512	988	0.1391	370.2	3.141
9	1551616	998	0.1226	370.4	3.174

Table 7
 Calculated values for GOX/P

Case	\dot{r}_{ave} (mm/s)	Thrust (N)	I _{sp} (s)	C* (m/s)	M _e
1	0.46	114	116	262	3.10
2	0.77	181	123	275	3.28
3	1.02	248	126	279	3.38
4	0.47	114	116	262	3.11
5	0.48	116	118	252	3.16
6	0.76	129	131	309	3.17
7	1.13	143	146	364	3.26
8	0.47	118	120	258	3.18
9	0.52	125	127	269	3.33

Table 8
 Calculated values for N2O/P

Case	\dot{r}_{ave} (mm/s)	Thrust (N)	I _{sp} (s)	C* (m/s)	M _e
1	0.34	103	105	234	2.80
2	0.46	162	110	237	3.01
3	0.67	221	113	233	3.14
4	0.38	99	101	217	2.72
5	0.42	97	99	212	2.69
6	0.66	120	122	268	3.01
7	0.93	136	139	300	3.11
8	0.46	101	103	222	2.77
9	0.52	102	104	224	2.79

The regression rate, thrust, specific impulse, characteristic velocity, and Mach number of the hybrid rocket model are presented in Table 7 and Table 8. Case 7 has the highest regression rate, specific impulse, and characteristic velocity for both oxidizers. While Case 3 has the highest thrust and exit Mach number. Therefore, the mass flow rate and temperature at the inlet have strongly affected the hybrid rocket performance. These parameters are far-reaching in rocketry design.

4.3 Effects on Regression Rate

Regression rate or also known as the rate at which the solid fuel is burned over time is affected by the oxidizer mass flow rate, pressure, temperature, and nozzle expansion ratio. The effects on the regression rate of hybrid rocket motor are illustrated in the graphical representation in this section.

The results are compared and validated with other published literature review. The validation has been made by comparing the trend of regression rate behaviour in the HRM [29-31].

4.3.1 Mass flow rate variation

The relationship between regression rate and fuel grain axial location with varying mass flow rate (0.10 kg/s for Case 1, 0.15 kg/s for Case 2, and 0.20 kg/s for Case 3) is shown in Figure 7. The regression rate can reach up to 1.8 mm/s for GOX/P and 1.2 mm/s for N2O/P for Case 3. The one with the lowest curve belongs to N2O/P for Case 1. The highest mass flow rate with the GOX oxidizer helps to produce a higher regression rate along the cylindrical paraffin fuel grain of the hybrid rocket motor compared to the N2O oxidizer.

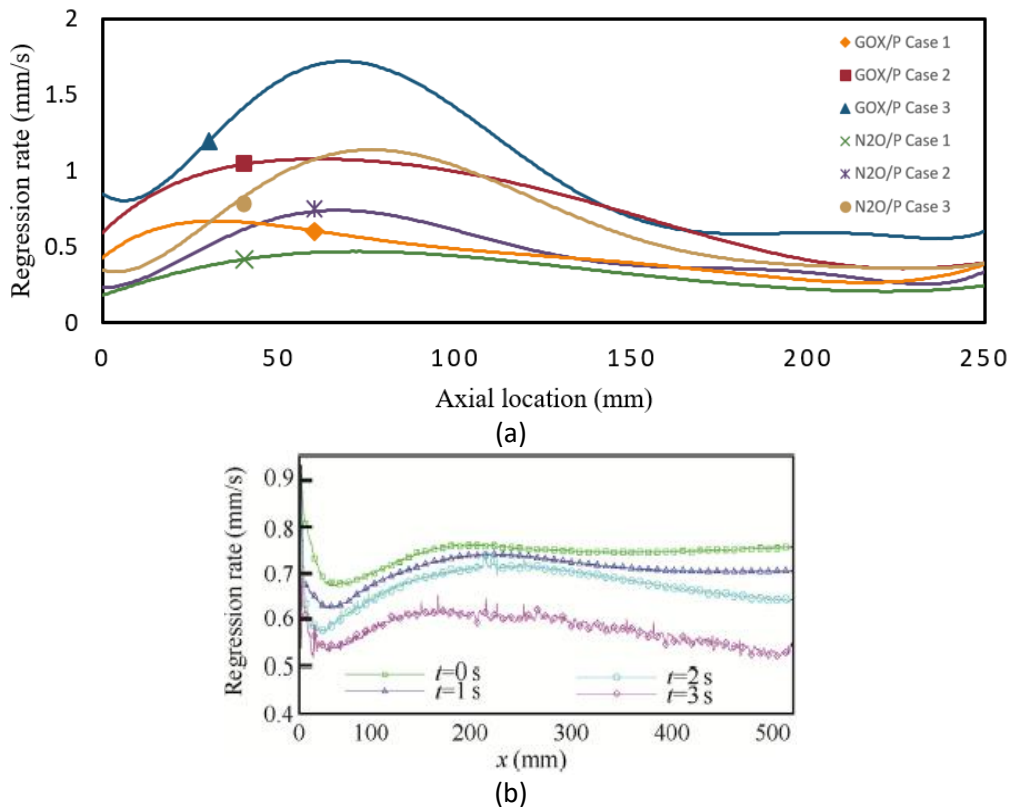


Fig. 7. (a) Regression rate versus axial location for mass flow rate effect, (b) Validation from Tian *et al.*, [29]

4.3.2 Pressure variation

There is a trivial change in regression rate values between Cases 1, 4, and 5 (2 atm for Case 1, 3 atm for Case 4, and 4 atm for Case 5) where the pressure at the hybrid rocket motor inlet is varied purposely to observe the effect of pressure on the regression rate. As a result, injection pressure does not have a significant effect on the regression rate of the hybrid rocket. Only two cases (GOX/P Case 5 and N2O/P Case 1) are selected for graphical representation of pressure effect on the regression rate as shown in Figure 8 due to the small effect. For GOX/P Case 5, the pressure is at 4 atm which is 2 atm higher than N2O/P Case 1. It can be observed that GOX/P Case 5 has more regression rates throughout the hybrid rocket fuel grain as compared to N2O/P Case 1.

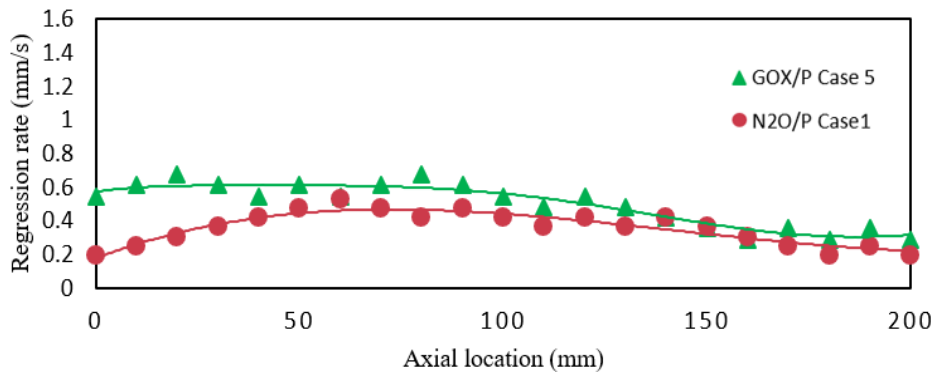


Fig. 8. Regression rate versus axial location for pressure effect

4.3.3 Temperature variation

Figure 9 represents the regression rate distribution along with the fuel grain axial location with three cases from each oxidizer. The inlet temperature for Cases 1, 6, and 7 (referring to Table 3) are 800 K, 1000 K, and 1200 K respectively. The highest average regression rate belongs to GOX/P with 1200 K inlet temperature. Case 7 has the lowest average regression rate with N2O/P. Increasing the inlet temperature can be one of the solutions for the low regression problem in a hybrid rocket motor.

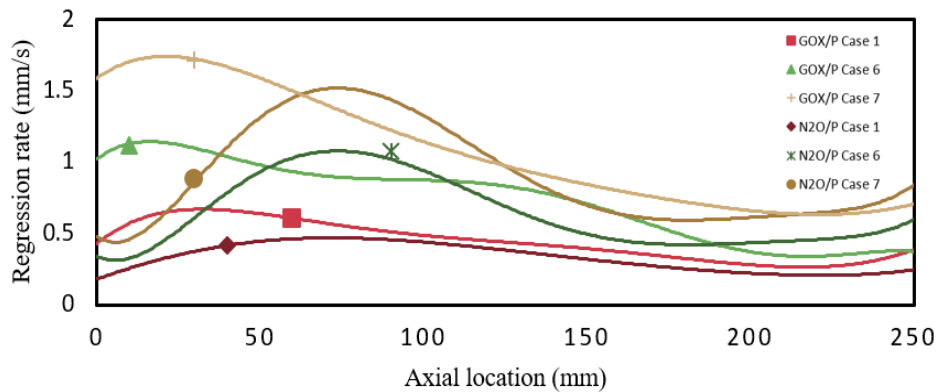


Fig. 9. Regression rate versus axial location for temperature effect

4.3.4 Nozzle expansion ratio variation

In this research, nozzle expansion ratio, or also known as throttling ratio exhibits a remarkable outcome on the hybrid rocket regression rate. The nozzle expansion ratio for Cases 1, 8, and 9 is 2.5, 3.0, and 3.5 respectively (referring to Table 3). There is a slight increase in the regression rate with the increase in the nozzle expansion ratio. The regression rate performance along the hybrid rocket fuel grain for the nozzle expansion ratio effect is presented in Figure 10. According to the National Aeronautics and Space Administration (NASA), the increase in the nozzle expansion ratio will increase the pressure chamber [12]. The pressure chamber obtained from the flow-fields indicates that the results are applicable. Nevertheless, this rise in the pressure chamber will significantly increase the requirements for the hybrid rocket engine weight and pumping.

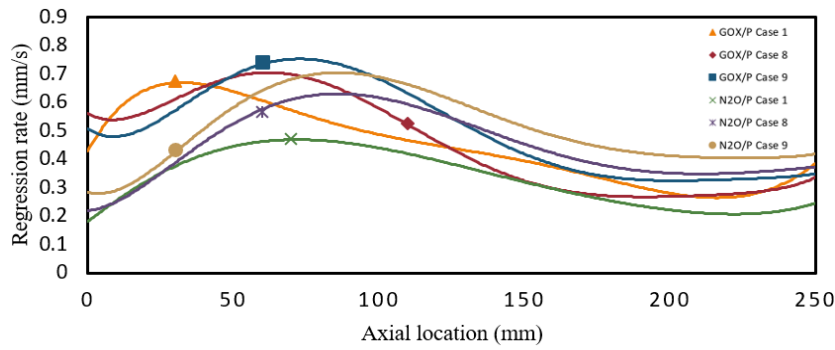


Fig. 10. Regression rate versus axial location for nozzle expansion ratio effect

4.4 Performance Difference between GOX and N2O

Figure 11 illustrates the relationship between regression rate behaviour and oxidizer mass flux for GOX/P and N2O/P hybrid rocket. The result indicates that the correlation between the regression rate and oxidizer mass flux is in line with the expression $\dot{r} = aGoxn$ which is commonly used in the engineering prediction.

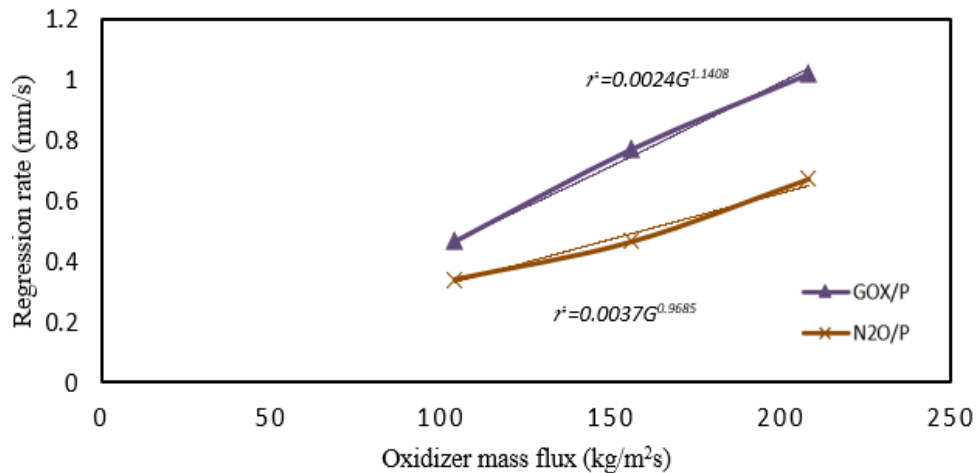


Fig. 11. Regression rate versus oxidizer mass flux

This approach is applied for Cases 1-9 and the relations are provided in Table 9. Note that the GOX/P expressions in terms of regression rate are leading in all cases. The GOX emits higher hot gas temperature compared to N2O as shown in Figure 12. The higher flame temperature provides more heat transferred to the grain surface, hence causes an increase in the regression rate. Validation of the regression rate for these two oxidizers shows the similar trend with 8.59% different with the research that has been made by Zhang *et al.*, [16] and Dinesh *et al.*, [17]. The result shows that the used of GOX will have higher regression rate compared with the N2O.

Table 9
 Summary of regression rate expressions

Propellant	GOX/P	N ₂ O/P
Mass flux	$\dot{r} = 0.0024G^{1.1408}$	$\dot{r} = 0.0037G^{0.9685}$
Mass flow rate	$\dot{r} = 6.5191\dot{m}^{1.1408}$	$\dot{r} = 3.0947\dot{m}^{0.9685}$
Pressure	$\dot{r} = 0.4428P^{0.0652}$	$\dot{r} = 0.2746P^{0.3062}$
Temperature	$\dot{r} = 2e^{-7}T^{2.1891}$	$\dot{r} = 2e^{-8}T^{2.4944}$
Expansion ratio	$\dot{r} = 0.3381\varepsilon^{0.3342}$	$\dot{r} = 0.1075\varepsilon^{1.2825}$

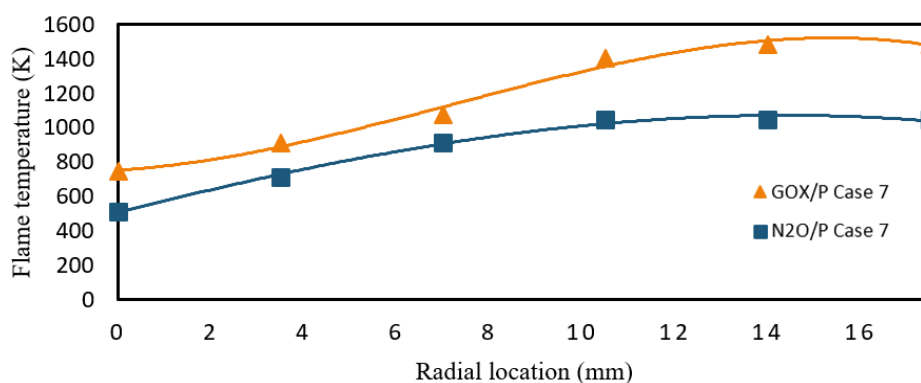


Fig. 12. Flame temperature versus radial location in the combustion chamber

5. Conclusions

In conclusion, the numerical results obtained from the modeling of hybrid rocket flow-fields are focusing on the enhancement of the regression rate. The Computational Fluid Dynamics analysis indicates that the mass-flow-inlet type of boundary conditions exhibit a consequential upshot on the hybrid rocket performance. The variation of the initial condition will affect the pressure exit, velocity exit, pressure chamber and wall heat flux, thus will also affect the calculation for HRM performance which used all the pressure exit, velocity exit, pressure chamber and wall heat flux value. Increasing 50% of the mass flow rate can increase up to 68% of the regression rate, 59% of thrust, 6% of specific impulse and exit Mach number, and 5% of characteristic velocity. As the oxidizer inlet temperature is increased by 200 K, a hybrid rocket can produce 65% more regression rate, 13% more thrust and specific impulse, 18% more characteristic velocity, and 3% more exit Mach number. There is only a slight increase in hybrid rocket performance when increasing the injection pressure and nozzle expansion ratio. The average hybrid rocket fuel regression rate with a propellant combination of gaseous oxygen and paraffin (GOX/P) was found higher value compared to nitrous oxide and paraffin (N2O/P).

Acknowledgement

This research was funded by a grant from Ministry of Higher Education of Malaysia (FRGS Grant 19-063-0671).

References

- [1] Archer, R. Douglas, and Maida Saarlax. *An introduction to aerospace propulsion*. Prentice Hall, 1996.
- [2] Liu, Lin-lin, Xiang He, Yin Wang, Ze-bin Chen, and Quan Guo. "Regression rate of paraffin-based fuels in hybrid rocket motor." *Aerospace Science and Technology* 107 (2020): 106269. <https://doi.org/10.1016/j.ast.2020.106269>
- [3] Bouziane, Mohammed, A. E. M. Bertoldi, Praskovia Milova, Patrick Hendrick, and Michel Lefebvre. "Performance comparison of oxidizer injectors in a 1-kN paraffin-fueled hybrid rocket motor." *Aerospace Science and Technology* 89 (2019): 392-406. <https://doi.org/10.1016/j.ast.2019.04.009>
- [4] Zhao, Bo, Nanjia Yu, Yufei Liu, Peng Zeng, and Jue Wang. "Unsteady simulation and experimental study of hydrogen peroxide throttleable catalyst hybrid rocket motor." *Aerospace Science and Technology* 76 (2018): 27-36. <https://doi.org/10.1016/j.ast.2018.02.008>
- [5] Yousef, Muntaha A., and M. Keith Hudson. "Thermal study of the decomposition of HTPB hybrid rocket fuel in the presence of azo-tetrazolate-based high nitrogen content high energy materials." *Journal of Thermal Analysis and Calorimetry* 134, no. 3 (2018): 1785-1797. <https://doi.org/10.1007/s10973-018-7490-6>
- [6] Naoumov, Viatcheslav I., Nidal A. Al Masoud, Kristine Sherman, Matthew Doolittle, Matthew Ziegler, and Daniel Thorne. "Study of the combustion of pure bio-derived fuels and bio-derived fuels with additives in hybrid propellant rocket engine." In *55th AIAA Aerospace Sciences Meeting*, p. 0833. 2017. <https://doi.org/10.2514/6.2017-0833>
- [7] Tian, Hui, Ruipeng Yu, Hao Zhu, Junfeng Wu, and Guobiao Cai. "Three-dimensional numerical and experimental

- studies on transient ignition of hybrid rocket motor." *Acta Astronautica* 140 (2017): 247-254. <https://doi.org/10.1016/j.actaastro.2017.08.022>
- [8] Franco, M., F. Barato, E. Paccagnella, M. Santi, A. Battiston, A. Comazzetto, and D. Pavarin. "Regression rate design tailoring through vortex injection in hybrid rocket motors." *Journal of Spacecraft and Rockets* 57, no. 2 (2020): 278-290. <https://doi.org/10.2514/1.A34539>
- [9] Mahottamananda, Sri Nithya, Nagarajan P. Kadiresh, and Yash Pal. "Regression Rate Characterization of HTPB-Paraffin Based Solid Fuels for Hybrid Rocket." *Propellants, Explosives, Pyrotechnics* 45, no. 11 (2020): 1755-1763. <https://doi.org/10.1002/prop.202000051>
- [10] Cai, Guobiao, Zeng Zhao, Bo Zhao, Yufei Liu, and Nanjia Yu. "Regression rate and combustion performance investigation on hybrid rocket motor with head-end swirl injection under high geometric swirl number." *Aerospace Science and Technology* 103 (2020): 105922. <https://doi.org/10.1016/j.ast.2020.105922>
- [11] Elanjickal, Silky, and Alon Gany. "Enhancement of the fuel regression rate in hybrid propulsion by expandable graphite additive." *Combustion Science and Technology* 192, no. 7 (2020): 1253-1273. <https://doi.org/10.1080/00102202.2020.1748017>
- [12] Oztan, Cagri, and Victoria Coverstone. "Utilization of additive manufacturing in hybrid rocket technology: A review." *Acta Astronautica* 180 (2021): 130-140. <https://doi.org/10.1016/j.actaastro.2020.11.024>
- [13] Sun, Xingliang, Hui Tian, Yuelong Li, Nanjia Yu, and Guobiao Cai. "Regression rate behaviors of HTPB-based propellant combinations for hybrid rocket motor." *Acta Astronautica* 119 (2016): 137-146. <https://doi.org/10.1016/j.actaastro.2015.11.015>
- [14] Okuda, Ryota, Kodai Komizu, Ayumu Tsuji, Takumi Miwa, Shuichi Yokobori, Kentaro Soeda, Landon T. Kamps, and Harunori Nagata. "Fuel Regression Characteristics of Axial-Injection End-Burning Hybrid Rocket Using Nitrous Oxide." In *AIAA Propulsion and Energy 2020 Forum*, p. 3753. 2020. <https://doi.org/10.2514/6.2020-3753>
- [15] Rashkovskiy, S. A., and S. E. Yakush. "Numerical simulation of low-melting temperature solid fuel regression in hybrid rocket engines." *Acta Astronautica* 176 (2020): 710-716. <https://doi.org/10.1016/j.actaastro.2020.05.002>
- [16] Zhang, Shuai, Fan Hu, and Weihua Zhang. "Numerical investigation on the regression rate of hybrid rocket motor with star swirl fuel grain." *Acta Astronautica* 127 (2016): 384-393. <https://doi.org/10.1016/j.actaastro.2016.06.017>
- [17] Dinesh, Mengu, Saideep Singh Rajput, and Rajiv Kumar. "Protrusion effect on the performance of hybrid rocket with liquefying and non-liquefying fuels." *Acta Astronautica* 178 (2021): 536-547. <https://doi.org/10.1016/j.actaastro.2020.09.039>
- [18] Vignesh, Bala, and Rajiv Kumar. "Effect of multi-location swirl injection on the performance of hybrid rocket motor." *Acta Astronautica* 176 (2020): 111-123. <https://doi.org/10.1016/j.actaastro.2020.06.029>
- [19] Petrarolo, Anna, Mario Kobald, and Stefan Schleichriem. "Understanding Kelvin-Helmholtz instability in paraffin-based hybrid rocket fuels." *Experiments in Fluids* 59, no. 4 (2018): 1-16. <https://doi.org/10.1007/s00348-018-2516-1>
- [20] Shrivastava, Aaditya. "Eco-Friendly Propellant for Hybrid Rocket Motor." In *Proceedings of the International Conference on Modern Research in Aerospace Engineering*, pp. 35-41. Springer, Singapore, 2018. https://doi.org/10.1007/978-981-10-5849-3_4
- [21] Thomas, James C., Christian Paravan, Jacob M. Stahl, Andrew J. Tykol, Felix A. Rodriguez, Luciano Galfetti, and Eric L. Petersen. "Experimental evaluation of HTPB/paraffin fuel blends for hybrid rocket applications." *Combustion and Flame* 229 (2021): 111386. <https://doi.org/10.1016/j.combustflame.2021.02.032>
- [22] Niknahad, Ali, and Abdolamir Bak Khoshnevis. "Numerical study and comparison of turbulent parameters of simple, triangular, and circular vortex generators equipped airfoil model." *Journal of Advanced Research in Numerical Heat Transfer* 8, no. 1 (2022): 1-18.
- [23] Sankaran, Venkateswaran. "Computational fluid dynamics modeling of hybrid rocket flowfields." *Progress in Astronautics and Aeronautics* 218 (2007): 323-350. <https://doi.org/10.2514/5.9781600866876.0323.0350>
- [24] Gudekote, Manjunatha, and Rajashekhar Choudhari. "Slip effects on peristaltic transport of Casson fluid in an inclined elastic tube with porous walls." *Journal of Advanced Research in Fluid Mechanics and Thermal Sciences* 43, no. 1 (2018): 67-80.
- [25] Hamrelaine, Salim, Fateh Mebarek-Oudina, and Mohamed Rafik Sari. "Analysis of MHD Jeffery Hamel flow with suction/injection by homotopy analysis method." *Journal of Advanced Research in Fluid Mechanics and Thermal Sciences* 58, no. 2 (2019): 173-186.
- [26] Alsadig, Ahmed, Hossin Omar, Suliman Alfarawi, and Azeldin El-sawi. "Mathematical Simulation of Baffled Shell and Tube Heat Exchanger utilizing Stream Analysis Model." *Journal of Advanced Research in Numerical Heat Transfer* 7, no. 1 (2021): 1-12.
- [27] Antoniou, Antonis, and Kazim Akyuzlu. "A physics based comprehensive mathematical model to predict motor performance in hybrid rocket propulsion systems." In *41st AIAA/ASME/SAE/ASEE Joint Propulsion Conference & Exhibit*, p. 3541. 2005. <https://doi.org/10.2514/6.2005-3541>

- [28] Y. Yoshida, "Numerical analysis of fuel regression rate in hybrid rocket motor," *AIAA J.*, pp. 1-140, 2018.
- [29] Tian, Hui, Yijie Li, and Peng Zeng. "Transient simulation of regression rate on thrust regulation process in hybrid rocket motor." *Chinese Journal of Aeronautics* 27, no. 6 (2014): 1343-1351.
<https://doi.org/10.1016/j.cja.2014.08.016>
- [30] Patnala, S., T. Chattaraj, and P. C. Joshi. "Combustion studies on paraffin wax in gaseous oxygen and nitrous oxide." *ARPN Journal of Engineering and Applied Sciences* 7, no. 7 (2012): 806-811.
- [31] Sankar, Vigneshwaran, Pavithra Muruges, and V. R. Sanal Kumar. "Wall Heat Flux Mapping of Liquid Rocket Thrust Chamber with Dual Impinging GH₂/GO₂ Jets." In *53rd AIAA/SAE/ASEE Joint Propulsion Conference*, p. 4766. 2017.
<https://doi.org/10.2514/6.2017-4766>